CRACK DEFLECTION AT AN INTERFACE BETWEEN DISSIMILAR ELASTIC MATERIALS

Ming-Yuan He†
Institute of Mechanics, Chinese Academy of Sciences, Beijing,
People's Republic of China

and

John W. Hutchinson
Division of Applied Sciences, Harvard University, Cambridge, MA 02138, U.S.A.

Abstract—A crack impinging an interface joining two dissimilar materials may arrest or may advance by either penetrating the interface or deflecting into the interface. The competition between deflection and penetration is examined in this paper when the materials on either side of the interface are elastic and isotropic. The energy release rate for the deflected crack is compared with the maximum energy release rate for a penetrating crack. The results can be used to determine the range of interface toughness relative to bulk material toughness which ensures that cracks will be deflected into the interface.

1. INTRODUCTION

In this paper several problems are analyzed which provide insight and quantitative information on the role an interface between dissimilar elastic materials plays when approached by a crack. At issue is whether a crack impinging on an interface will pass through the interface or be deflected into the interface. Such questions are of importance, for example, in the design of the interface between fiber and matrix in fiber reinforced ceramic composites where it is desired that any matrix crack approaching a fiber deflect along the interface, thereby allowing the fiber to survive. The results from this study provide estimates of the relative toughness of the interface to that of the material on the uncracked side of the interface necessary to ensure that a crack will deflect into the interface rather than penetrate it.

The four sets of problems analyzed are shown in Fig. 1. In set A, a symmetrically loaded, semi-infinite main crack impinges the interface at a right angle. The three problems analyzed (problems A1, A2 and A3) permit an assessment of the competition between penetration of the interface and deflection. Set B in Fig. 2 addressed the same competition when the main crack impinges on the interface at an oblique angle. An unusual feature of the oblique problem for the main crack (with $a = 0$) is the fact that there is a *single* dominant mode of deformation at the crack tip when the materials across the interface are dissimilar. Thus the asymptotic behavior at the crack tip is influenced by the remote loads only through a single stress intensity factor. The competition between penetration and deflection as posed in problems B1 and B2 does not depend on the nature of the remote loads in a strict asymptotic sense when the branch length a is arbitrarily small compared to the length of the main crack.

A consequence of the existence of a single dominant mode of the main crack impinging the interface at an oblique angle is a tendency for a crack approaching the interface to turn either into or away from the interface, depending on the relative stiffnesses of the materials on either side of the interface. In problem C in Fig. 1 the behavior of a straight wedge-loaded, semi-infinite crack is determined as the crack approaches the interface. This problem gives further insight into the tendency of a crack to curve into or away from the interface when it approaches at an oblique angle. Finally, in problems D1 and D2 the competition between penetration through the interface or deflection into it is analyzed for an oblique

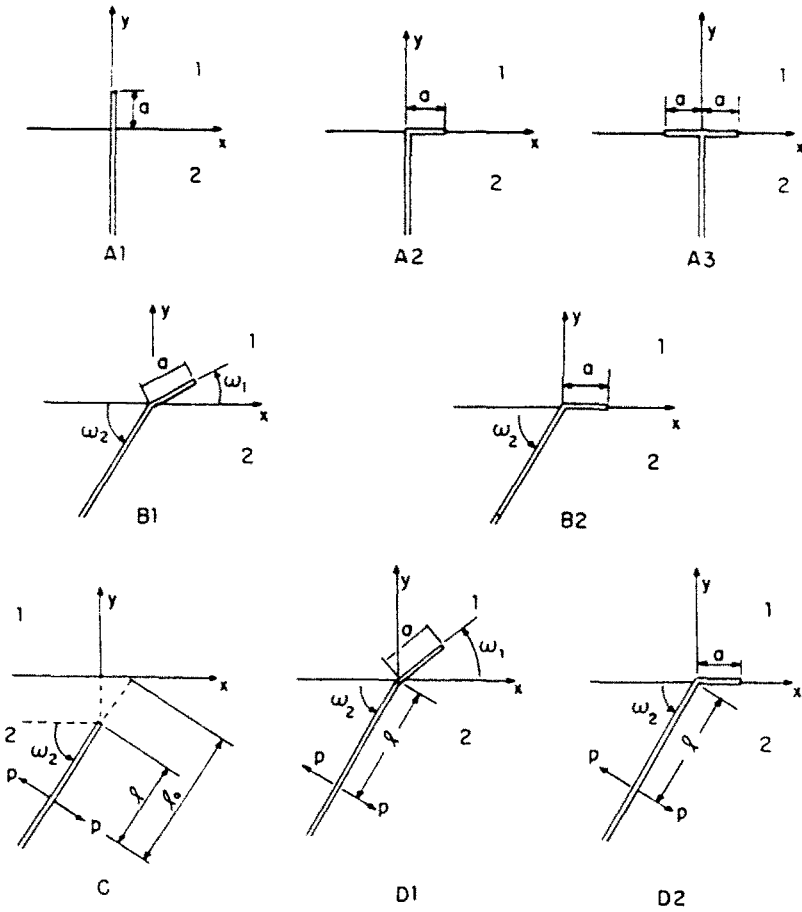† Visiting Scholar, Harvard University, August 1987–August 1988.
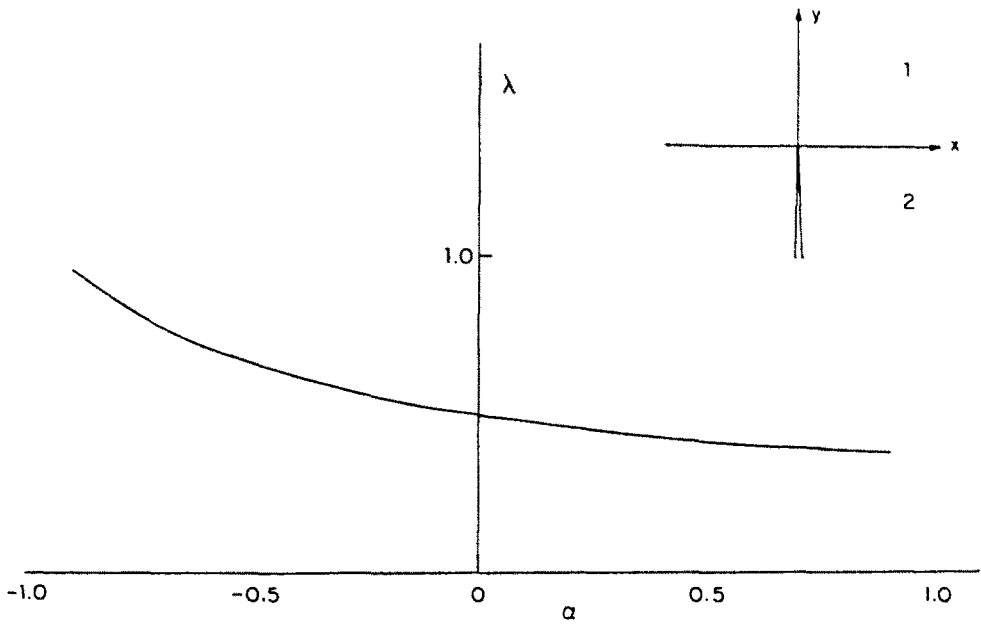
Fig. 1. Crack geometries.

Fig. 2. Stress singularity exponent for $\beta = 0$.

wedge-loaded crack. These problems are solved for *finite* values of a/l where l is the distance of the wedge loads from the interface. The behavior as $a/l \to 0$ is discussed in relation to the problems in set B.

There are a number of earlier studies which analyze details of crack penetration and/or deflection at an interface without specifically focussing on the competition between the two modes of cracking. The solution procedures used in the present study are similar to, or extensions of, the integral equation methods used in these earlier papers. Cook and Erdogan (1972) and Erdogan and Biricikoglu (1973) investigate the behavior of a crack penetrating the interface at right angles. Goree and Venezia (1977) analyze several problems involving penetration and deflection for a main crack impinging the interface at right angles. Additional work along these same lines is reported by Lu and Erdogan (1983). The tendency for a crack approaching an interface or a free surface at an oblique angle to be deflected one way or the other has been elucidated by studies of Erdogan and Arin (1975) and more recently by Lardner *et al.* (1989).

In all cases the materials on either side of the interface are taken to be elastic and isotropic with shear modulus μ_i and Poisson's ratio ν_i where $i = 1$ and 2 correspond to the arrangement shown in Fig. 1. For the plane strain, traction boundary value problems considered, the solution variables of interest depend on only two non-dimensional combinations of the material parameters. These are the Dundurs' (1969) parameters

$$\alpha = [\mu_1(1-\nu_2)-\mu_2(1-\nu_1)]/[\mu_1(1-\nu_2)+\mu_2(1-\nu_1)] \tag{1}$$

$$\beta = [\mu_1(1-2\nu_2)-\mu_2(1-2\nu_1)]/[\mu_1(1-\nu_2)+\mu_2(1-\nu_1)]. \tag{2}$$

The first parameter is most readily interpreted when expressed as $\alpha = (\bar{E}_1 - \bar{E}_2)/(\bar{E}_1 + \bar{E}_2)$ where $\bar{E} = E/(1-\nu^2)$ is the plane strain tensile modulus. The solutions to the four sets of problems are presented and discussed in the following sections. The problems are formulated and analyzed in the Appendices.

2. DEFLECTION VERSUS PENETRATION FOR A CRACK PERPENDICULAR TO THE INTERFACE (PROBLEMS A)

In the set A of problems the semi-infinite reference crack with $a = 0$ is perpendicular to the interface with its tip at the interface. A symmetric loading with respect to the crack plane is applied and the traction ahead of the crack in material 1 is characterized by

$$\sigma_{xx}(0, y) = k_1(2\pi y)^{-\lambda} \tag{3}$$

where λ is real and depends on α and β according to (Zak and Williams, 1963)

$$\cos \lambda\pi = \frac{2(\beta-\alpha)}{1+\beta}(1-\lambda)^2 + \frac{\alpha+\beta^2}{1-\beta^2}.$$

A plot of λ as a function of α for $\beta = 0$ is shown in Fig. 2. The amplitude factor k_1 is proportional to the applied load. Explicit knowledge of k_1 is not needed here. The reference crack is imagined to advance in the three ways indicated in Fig. 1: one by penetration straight through the interface (A1) and two by deflection into the interface (A2 and A3).

In the case of penetration, the stress state at the advancing tip is pure mode I. By dimensional considerations its stress intensity factor must depend on k_1 and a according to

$$K_1 = c(\alpha, \beta)k_1 a^{1/2-\lambda} \tag{4}$$

where c is dimensionless. The energy release rate is

$$\mathcal{G}_p = \frac{1-v_1}{2\mu_1} K_1^2 = \frac{1-v_1}{2\mu_1} c^2 k_1^2 a^{1-2\lambda}. \tag{5}$$

The traction on the interface directly ahead of the right-hand tip of either of the deflected cracks (A2 or A3) is characterized by (Rice, 1988)

$$\sigma_{yy}(x,0)+i\sigma_{xy}(x,0) = (K_1+iK_2)(2\pi r)^{-1/2}r^{i\varepsilon} \tag{6}$$

where $r = x-a$, $i = \sqrt{-1}$, and

$$\varepsilon = \frac{1}{2\pi} \ln \left(\frac{1-\beta}{1+\beta}\right). \tag{7}$$

In these cases, dimensional considerations require

$$K_1+iK_2 = k_1 a^{1/2-\lambda}[d(\alpha,\beta)a^{i\varepsilon}+e(\alpha,\beta)a^{-i\varepsilon}] \tag{8}$$

where d and e are dimensionless complex valued functions of α and β. The energy release rate of the deflected crack is

$$\mathcal{G}_d = [(1-v_1)/\mu_1+(1-v_2)/\mu_2](K_1^2+K_2^2)/(4\cosh^2 \pi\varepsilon) \tag{9}$$

where

$$K_1^2+K_2^2 = k_1^2 a^{1-2\lambda}[|d|^2+|e|^2+2R_e(de)]. \tag{10}$$

In each of the three cases the energy release rate goes to zero or becomes unbounded as $a \to 0$ depending on whether λ is less than or greater than $1/2$. But the dependence of $\mathcal{G}$ on a is very weak since λ differs only slightly from $1/2$ except for $\alpha < -0.7$ (cf. Fig. 2). More importantly, the ratio $\mathcal{G}_d/\mathcal{G}_p$ is independent of a (and k_1) and is given by

$$\mathcal{G}_d/\mathcal{G}_p = [(1-\beta^2)/(1-\alpha)][|d|^2+|e|^2+2R_e(de)]/c^2. \tag{11}$$

Thus the *relative* tendency of a crack to be deflected by the interface or to pass through it can be assessed using this ratio.

Integral equation methods have been used to solve for the function $c(\alpha,\beta)$ for the case of the penetrating crack and for $d(\alpha,\beta)$ and $e(\alpha,\beta)$ for the two cases involving deflected cracks. The details of the solution procedures are given in Appendices I and II. The ratio $\mathcal{G}_d/\mathcal{G}_p$ is plotted as a function of α in Fig. 3 for $\beta = 0$ for each case. The effect of β has not been systematically explored since it is felt that α is the more important of the two parameters. In any case, the effect of β on the ratio is not expected to be large, as was seen in a similar problem (He and Hutchinson, 1989). Note, for example, that β appears explicitly in (11) only to order β^2. The relative amounts of K_1 and K_2 at the right-hand tip of the deflected cracks are presented in Fig. 4 using the measure $\psi = \tan^{-1}(K_2/K_1)$.

Let $\mathcal{G}_{ic}$ be the toughness of the interface (which may depend on ψ) and let $\mathcal{G}_c$ be the mode I toughness of material 1. The impinging crack is likely to be deflected into the interface if

$$\mathcal{G}_{ic}/\mathcal{G}_c < \mathcal{G}_d/\mathcal{G}_p \tag{12}$$

since then the condition for propagation in the interface will be met at a lower load than that for penetration across the interface. Conversely, the crack will tend to penetrate the interface when the inequality is reversed. The deflected crack branching to one side (as opposed to the crack with the double branch) generally controls the condition for deflection into the interface since it corresponds to the highest ratio $\mathcal{G}_d/\mathcal{G}_p$, although the double branching crack could control if $\mathcal{G}_{ic}$ depends strongly on ψ. For α not too different from
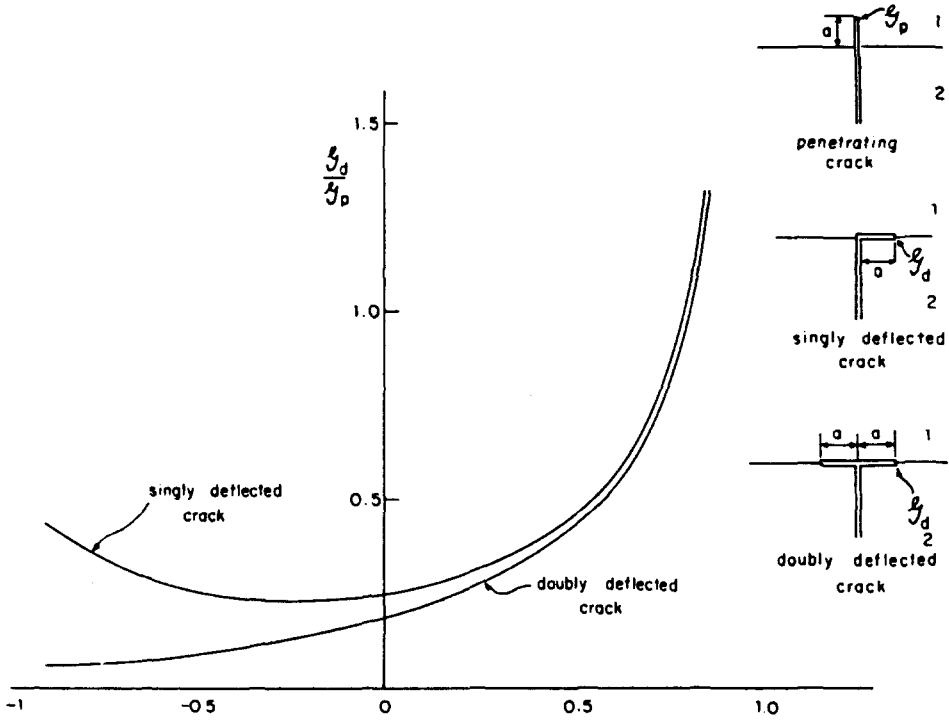
Fig. 3. Ratio of energy release rate of deflected crack to penetrating crack at same amount of crack advance a.

zero, the critical ratio is approximately $1/4$. It increases to approximately $1/2$ when $\alpha = 1/2$, corresponding to a plane strain tensile modulus of material 1 being three times that of material 2.

The analysis has not addressed the question of the load level required for the crack to deflect into the interface or to penetrate it. Rather, it has exploited the fact that the energy release rates of the competing crack trajectories depend on crack advance a, in exactly the same way. Thus the relative energy release rates can be unambiguously determined and used to assess which of the competing trajectories will be selected. When $\lambda < 1/2$ it is
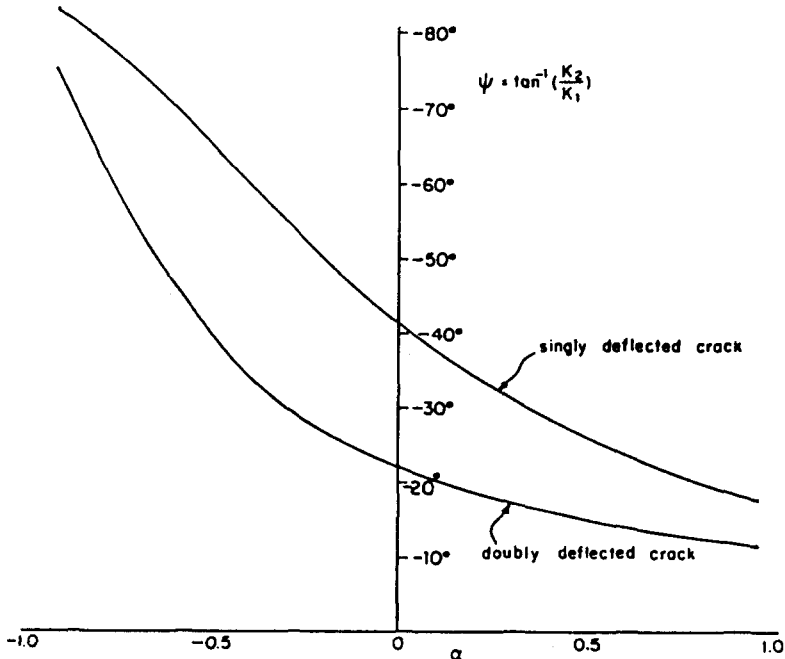

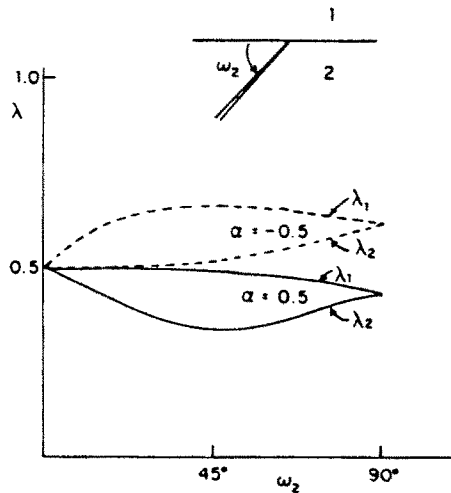Fig. 4. Combination of interface stress intensity factors at right-hand tip of deflected crack.

Fig. 5. Stress singularity exponents for crack impinging interface at an oblique angle ($\beta = 0$).

necessary to invoke intrinsic flaws in either the interface or in material 1 for the crack to grow from the tip when $a = 0$. The condition (12) implicitly assumes these intrinsic flaws of comparable size. The above conclusions are also drawn under the assumption that the crack approaches the interface quasistatically. Dynamic effects may alter the conclusions somewhat when the impinging crack is traveling at a significant fraction of the elastic wave speed.

3. CRACK TERMINATING AT AN INTERFACE AT AN OBLIQUE ANGLE

There is a peculiarity to the problem of a crack impinging on an interface at an oblique angle which makes a discussion of the relative tendency for deflection or penetration somewhat more complicated than the case of the perpendicularly impinging crack. The peculiarity concerns the nature of the singular stress fields for an oblique crack terminating at the interface with the geometry shown in the insert in Fig. 5.

For a homogeneous material ($\alpha = \beta = 0$) or for the crack making a right angle with the interface between two different materials ($\omega_1 = \pi/2$), the most singular stress fields of physical interest at the tip can be written as

$$\sigma_{ij} = k_1 r^{-\lambda} \sigma_{ij}^{\rm I}(\theta) + k_{\rm II} r^{-\lambda} \sigma_{ij}^{\rm II}(\theta) \tag{13}$$

where $\lambda = 1/2$ for the homogeneous material and λ is given in Fig. 2 for ($\omega_1 = \pi/2$). In these cases, the eigenvalue problem for the exponent λ has a double root yielding two linearly independent fields $\sigma_{ij}^{\rm I}$ and $\sigma_{ij}^{\rm II}$ which can be taken to be symmetric and anti-symmetric relative to the crack plane. When the crack lies on the interface ($\omega_1 = 0$) the eigenvalue is also double with $\lambda = 1/2$ when $\beta = 0$.

For values of ω_1 between 0 and $\pi/2$ the eigenvalue problem no longer has double roots when the materials are dissimilar. Instead of (13), the two most singular fields of interest are

$$\sigma_{ij} = k_1 r^{-\lambda_1} \sigma_{ij}^{(1)}(\theta) + k_2 r^{-\lambda_2} \sigma_{ij}^{(2)}(\theta) \tag{14}$$

where λ_1 and λ_2 are real for $\beta = 0$. Corresponding to each eigenvalue is only one eigenfunction instead of two. The two exponents λ_1 and λ_2 are plotted as a function of ω_2 in Fig. 5 for $\alpha = \pm 0.5$ with $\beta = 0$. If λ_1 is identified as the larger of two exponents, the dominant singular field is
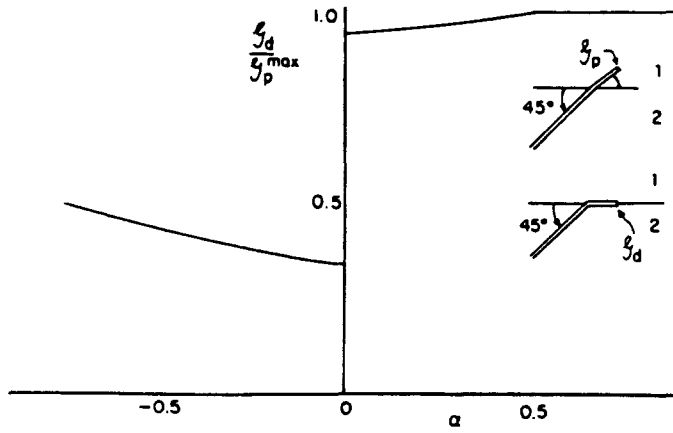
Fig. 6. Ratio of ratio of energy release rate of deflected crack to maximum energy release rate of penetrating crack at same a for asymptotic problem characterized by (15) when $a \to 0$ ($\beta = 0$).

$$\sigma_{ij} = k_1 r^{-\lambda_1} \sigma_{ij}^{(1)}(\theta) \tag{15}$$

where $\sigma_{ij}^{(1)}(\theta)$ is a mixed mode θ-variation which depends on ω_2 and α.

Thus, unlike the problems mentioned above—indeed, unlike most linear crack problems—the oblique crack terminating at an interface has a *fixed* mixed mode (i.e. a fixed θ-variation) independent of the remote loading combinations acting on the body. The zone of dominance of (15) may be very small and must vanish as α and β vanish since then the two-term representation (13) holds. Similarly, dominance must vanish as $\omega_1 \to 0$ or $\pi/2$. In spite of the limited range of dominance expected for (15), we have considered the competition between penetration and deflection at an interface for an oblique crack where (15) specifies the dominant field at the tip of the main crack. These results are discussed in the next section. In the last two sections, we circumvent the issue of limited dominance of the asymptotic problem by analyzing an oblique crack under a specific wedge-loading.

4. ASYMPTOTIC LIMITS FOR DEFLECTION VERSUS PENETRATION FOR AN OBLIQUE CRACK (PROBLEMS B)

In problems B1 and B2 (cf. Fig. 1) the dominant singularity field (15) is imposed as the remote field on the main semi-infinite crack. The competition between penetration of the interface and deflection into the interface parallels that discussed in Section 2 for the perpendicular crack under symmetric load. Now, however, the direction taken by the crack penetrating into material $1, \omega_1$, must be determined. The direction chosen will be that which maximizes the energy release rate.

The stress intensity factors at the tip of the penetrating crack are related to k_1 and a by

$$K_1 + iK_{11} = c(\alpha, \omega_1, \omega_2)k_1 a^{1/2 - \lambda_1} \tag{16}$$

where c is a dimensionless complex-valued function and attention will be focussed on material combinations with $\beta = 0$. The energy release rate of the penetrating crack is

$$\mathcal{G}_p = \frac{1 - \nu_1}{2\mu_1} |c|^2 k_1^2 a^{1 - 2\lambda_1}. \tag{17}$$

The maximum energy release rate with respect to ω_1 for fixed a is denoted by $\mathcal{G}_p^{max}$. The interface stress intensity factors of the deflected crack can be expressed as (8) with $\varepsilon = 0$ and k_1 and λ replaced by k_1 and λ_1, respectively. The ratio of the two energy release rates is again independent of a and is given by

$$\mathcal{G}_d / \mathcal{G}_p^{max} = (1 - \alpha)^{-1} [|d|^2 + |e|^2 + 2R_e(de)]/|c|^2. \tag{18}$$

Numerical results for this ratio as a function of α are shown in Fig. 6 for the case where

$\omega_2 = 45$. When material 1 is stiff compared to material 2 ($x > 0$) the maximum energy release rate of the penetrating crack is only slightly larger than that of the deflected crack. In fact, when x is greater than about 0.5 the maximum energy release rate of the penetrating crack is attained for $\omega_1 \to 0$ so that the critical penetrating crack coincides with the deflecting crack. When material 1 is the more compliant material the energy release rate of the penetrating crack significantly exceeds that of the deflecting crack.

The discontinuity in $\mathcal{G}_d/\mathcal{G}_p^{max}$ in Fig. 6 at $x = 0$ is associated with exchange in roles of (λ_1, λ_2) and $(\sigma^{(1)}(\theta), \sigma^{(2)}(\theta))$ in (14) as x changes sign. The θ-variation of the dominant singularity field (15) changes discontinuously as x changes sign. As has already been mentioned, the dominance of the single field (15) vanishes as $x \to 0$.

We proceed from here by considering the specific wedge-opening loading indicated in problems C and D in Fig. 1. One consequence of a *single* dominated mixed mode for the crack terminating at the interface is that a straight crack approaching the interface will necessarily experience a mixed mode at its tip. This is illustrated by example in the next section where its implications are discussed. In Section 6 we reconsider the competition between penetration and deflection for the oblique crack under the wedge loading for finite values of a/l.

5. STRAIGHT CRACK UNDER WEDGE LOADING APPROACHING AN INTERFACE AT AN OBLIQUE ANGLE (PROBLEM C)

With the tip of the crack in material 2, the near tip fields are a combination of modes I and II. Here we examine the history of K_I and K_{II} for the semi-infinite, *straight* crack loaded by the opening wedge forces per unit thickness P shown as C in Fig. 1. The solution for the stress intensity factors can be written as

$$K_I + iK_{II} = cPl^{-1/2} \tag{19}$$

where l is the distance of the tip from the loads and where c is a dimensionless, complex function of x, β, ω_2 and l/l_0. When l is small compared to l_0 the crack tip is in mode I with the well-known result

$$K_I \to \left(\frac{2}{\pi}\right)^{1/2} Pl^{-1/2} \quad \text{for} \quad l/l_0 \ll 1. \tag{20}$$

As l increases the crack tip interacts with the interface and some amount of mode II is induced. Plots of K_{II}/K_I as a function of l/l_0 are given in Fig. 7 for three angles of approach ($\omega_2 = 30$, 45 and 60) for two material combinations ($x = 0.5$ and $\alpha = -0.5$, each with $\beta = 0$). These results have been computed using an integral equation approach given in Appendix B.

When the crack approaches a more compliant material across the interface ($x < 0$) K_{II} become negative, although it is very slightly positive for an initial range of l/l_0. If it were free to curve following a path with K_{II} always zero, the crack would curve toward the interface since the straight crack has $K_{II} < 0$. Conversely, when the straight crack approaches a stiffer material across the interface ($x > 0$), K_{II} becomes positive suggesting that an actual crack trajectory satisfying $K_{II} = 0$ would curve away from the interface. Conjectured trends are sketched in Fig. 8. Similar conclusions have been drawn in the studies of Erdogan and Arin (1975) and Lardner *et al.* (1989).

The variation of the energy release rate

$$\mathcal{G} = \frac{(1 - v_2)}{2\mu_2} |c|^2 \frac{P^2}{l} \tag{21}$$

with l/l_0 is shown in Fig. 9 for $\omega_2 = 60$ and for $x = 0$ and ± 0.5 with $\beta = 0$. These variations reflect the behavior that is well-known for a crack approaching an interface at right angles.
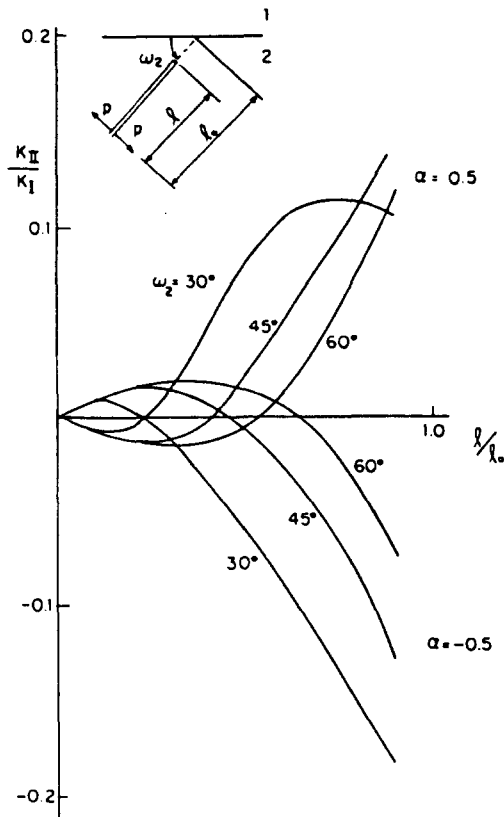
Fig. 7. Ratio of K_{II} to K_I for wedge loaded straight crack approaching the interface at several angles.
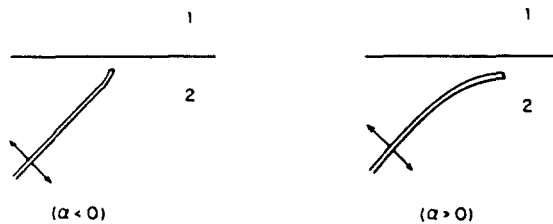

Fig. 8. Conjectured trends for crack approaching an interface.

When the material across the interface is stiffer than that where the crack resides ($\alpha > 0$), $\mathscr{G}$ must drop to zero as the interface is approached. But note from Fig. 5 that λ_1 is only very slightly smaller than $1/2$ for $\omega_2 = 60°$ and $\alpha = 0.5$, and thus $\mathscr{G}$ has not yet started to drop steeply even when $l/l_0 = 0.95$. When $\alpha = -0.5$, corresponding to a more compliant material across the interface, $\lambda_1 = 0.67$ and the increase in $\mathscr{G}$ as the interface is approached is more dramatic.

6. DEFLECTION VERSUS PENETRATION OF A WEDGE-LOADED CRACK IMPINGING AN INTERFACE AT AN OBLIQUE ANGLE (PROBLEMS D)

The main semi-infinite crack in Set D in Fig. 1 is subject to opening wedge loads, P, a distance, l, from the interface along the crack line. Competition between penetration (D1) and deflection (D2) is analyzed. As noted in the previous section an oblique crack under the wedge-opening loading is not expected to approach the interface as a straight crack. Nevertheless, the problems analyzed in this section should give further insight into the crack deflection process. Moreover, the results of this section place the behavior of the perpendicular crack in perspective.

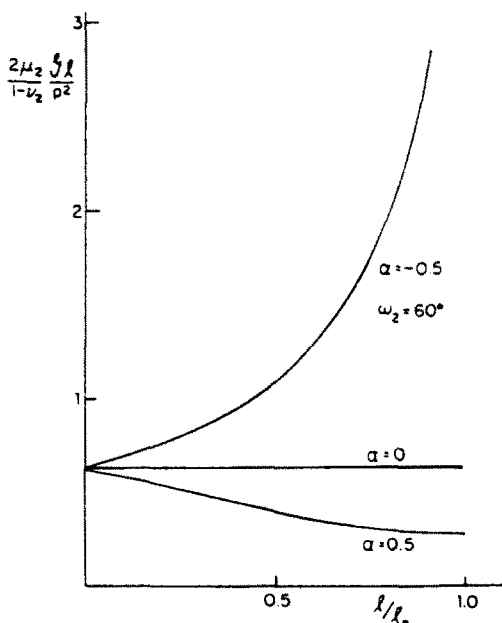The solution for the stress intensity factors in problem D1 can be written as

Fig. 9. Normalized energy release rate for straight crack approaching an interface at $\omega_2 = 60$
$(\beta = 0)$.

$$K_1 + iK_{11} = c(\alpha, \omega_1, \omega_2, a/l)Pl^{-1/2} \qquad (22)$$

where c is a dimensionless complex-valued function of the arguments indicated (β is again taken to be zero). The energy release rate is

$$\mathcal{G}_p = \frac{(1 - v_1)}{2\mu_1}|c|^2 \frac{P^2}{l}. \qquad (23)$$

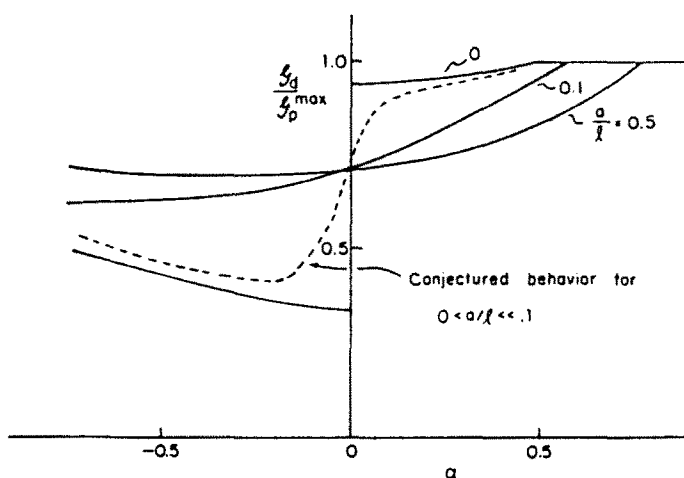The maximum value of $\mathcal{G}_p$ with respect to ω_1 for fixed a/l is denoted by $\mathcal{G}_p^{max}$.

Fig. 10. Ratio of energy release rate of deflected crack to maximum energy release rate of penetrating crack at same a for $\omega_2 = 45$ and $\beta = 0$.
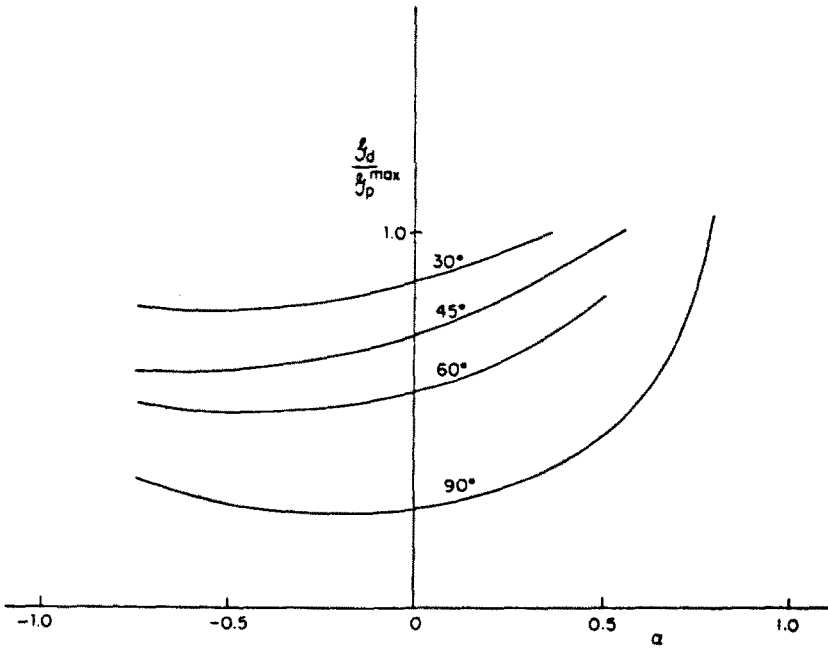
$$\frac{\mathcal{G}_d}{\mathcal{G}_p^{max}}$$

Fig. 11. Ratio of energy release rate of deflected crack to maximum energy release rate of penetrating crack at same a for wedge loaded crack with $\omega_2 = 30^\circ, 45^\circ, 60^\circ$; $a/l = 0.1$ and $\beta = 0$. The curve for $\omega_2 = 90^\circ$ is from Fig. 3.

With $\beta = 0$, the interface intensity factors for the deflected crack can be expressed in a manner similar to (22), i.e.

$$K_1 + iK_2 = d(\alpha, \omega_2, a/l) P l^{-1/2}. \tag{24}$$

The energy release rate of the deflected crack, $\mathcal{G}_d$, is again given by (9) (with $\varepsilon = 0$) where $K_1^2 + K_2^2 = |d|^2 P^2/l$.

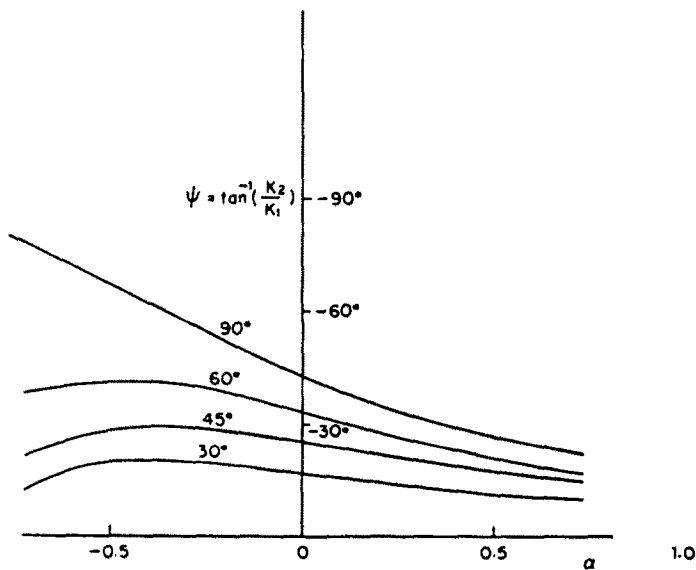The ratio of the competing energy release rates is

$$\psi = \tan^{-1}\left(\frac{K_2}{K_1}\right)$$

Fig. 12. Combination of interface stress intensity factors at tip of deflected crack for $\omega_2 = 30^\circ, 45^\circ, 60^\circ$ and 90°.

$$\mathscr{G}_d/\mathscr{G}_p^{\max} = (1-\alpha)^{-1}|d|^2/|c|^2. \tag{25}$$

This ratio is plotted as a function α for $\omega_2 = 45°$ in Fig. 10 for $a/l = 0.5$ and 0.1; the asymptotic limit of Section 4 for $a/l \to 0$ is also included, taken from Fig. 6. Equation (25) has a finite limit as $a \to 0$, and we believe that this limit must be the asymptotic result of Section 4. We have not attempted to compute the ratio (25) for values of a/l smaller than 0.1. However, we conjecture that results for significantly smaller a/l will approach the asymptotic limit in the manner indicated in Fig. 10.

Curves of $\mathscr{G}_d/\mathscr{G}_p^{\max}$ as a function of α are shown in Fig. 11 for $a/l = 0.1$ and $\omega_2 = 30°$, 45, and $60°$. Included also is the curve from Fig. 3 for the singly deflected crack with $\omega_2 = 90$. The associated measure ψ of the relative combination of the stress intensity factors of the deflected crack is given in Fig. 12. As one would expect intuitively, the competition between deflection and penetration becomes more favorable to deflection the more oblique is the crack impinging the interface. If one desires to design the toughness of an interface such that a crack of any orientation will be deflected, then the results for the perpendicularly impinging crack ($\omega_2 = 90$) control the choice of interface toughness. For α-values in the range of -0.5 to about 0.25 the toughness of the interface (measured in energy units) must be less than about one quarter of the toughness of the material across the interface if all cracks are to be deflected.

REFERENCES

Cook, T. S. and Erdogan, F. (1972). Stresses in bonded materials with a crack perpendicular to the interface. *Int. J. Engng Sci.* **10**, 677-697.
Dundurs, J. (1969). Edge-bonded dissimilar orthogonal elastic wedges. *J. Appl. Mech.* **36**, 650-652.
Erdogan, F. and Arin, K. (1975). Half plane and a strip with an arbitrary located crack. *Int. J. Fract.* **11**, 191-204.
Erdogan, F. and Biricikoglu, V. (1973). Two bonded half planes with a crack going through the interface. *Int. J. Engng Sci.* **11**, 745-766.
Goree, J. G. and Venezia, W. A. (1977). Bonded elastic half-planes with an interface crack and a perpendicular intersecting crack that extends into the adjacent material. *Int. J. Engng Sci.* **15**, Part I, 1-17; Part II, 19-27.
He, M. Y. and Hutchinson, J. W. (1989). Kinking of a crack out of an interface. To be published in *J. Appl. Mech.* (in press).
Hein, V. L. and Erdogan, F. (1971). Stress singularities in a two material wedge. *Int. J. Fract. Mech.* **7**, 317-330.
Lu, M-C. and Erdogan F. (1983). Stress intensity factors in two bonded elastic layers containing cracks perpendicular to and on the interface. *Engng Fract. Mech.* **18**, Part I, 491-506; Part II, 507-528.
Lardner, T. J., Ritter, J. E., Shiao, M. L. and Lin, M. R. (1989). Behavior of cracks near free surfaces and interfaces. To be published.
Rice, J. R. (1988). Elastic fracture concepts for interfacial cracks. *J. Appl. Mech.* **55**, 98-103.
Zak, A. R. and Williams, M. L. (1963). Crack point singularities at a bi-material interface. *J. Appl. Mech.* **30**, 142-143.

APPENDIX A: INTEGRAL EQUATIONS

In this Appendix we set up the integral equations for the plane strain problem specified in Fig. A1, which is representative of several of the various problems.

Let $a_r(\eta_1)$ and $a_\theta(\eta_1)$ be the r and θ components of an edge dislocation located on the radial line $\theta = \omega_1$ at $Z_1 = \eta_1 e^{i\omega_1}$, and let $b_r(\eta_2)$ and $b_\theta(\eta_2)$ be the r and θ components of an edge dislocation located on the radial line $\theta = \pi + \omega_2$ at $Z_2 = \eta_2 e^{i(\pi+\omega_2)}$. The stresses induced by a dislocation can be obtained using the Muskhelishvili method and are given as follows.
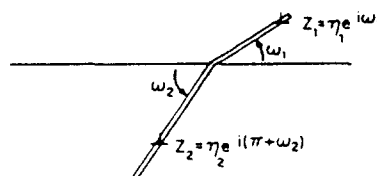

Fig. A1. Geometry conventions.

The stress components $\sigma_{\theta\theta}$ and $\sigma_{r\theta}$ at a point $Z = t_2 e^{i(\pi+\omega_2)}$ on the radial line $\theta = \pi + \omega_2$ induced by the dislocation at $Z_2 = \eta_2 e^{i(\pi+\omega_2)}$ are given by

$$\sigma_{\theta\theta} + i\sigma_{r\theta} = 2\bar{B}(\eta_2)\, e^{i\omega_2}\, (\eta_2 - t_2) + B(\eta_2)G_1(\eta_2, t_2) + \bar{B}(\eta_2)G_2(\eta_2, t_2). \tag{A1}$$

Similarly, the stresses at a point $Z = t_1 e^{i\omega_1}$ on the radial line $\theta = \omega_1$ induced by the dislocation at $Z_2 = \eta_2 e^{i(\pi+\omega_2)}$ are given by

$$\sigma_{\theta\theta} + i\sigma_{r\theta} = B(\eta_2)F_3(\eta_2, t_1) + \bar{B}(\eta_2)F_4(\eta_2, t_1). \tag{A2}$$

The stresses at a point $Z = t_1 e^{i\omega_1}$ on the radial line $\theta = \omega_1$ induced by the dislocation at $Z_1 = \eta_1 e^{i\omega_1}$ are given by

$$\sigma_{\theta\theta} + i\sigma_{r\theta} = 2\bar{A}(\eta_1)\, e^{i\omega_1}\, (t_1 - \eta_1) + A(\eta_1)F_1(\eta_1, t_1) + \bar{A}(\eta_1)F_2(\eta_1, t_1). \tag{A3}$$

The stresses at a point $Z = t_2 e^{i(\pi+\omega_2)}$ on the radial line $\theta = \pi + \omega_2$ induced by the dislocation at $Z_1 = \eta_1 e^{i\omega_1}$ are given by

$$\sigma_{\theta\theta} + i\sigma_{r\theta} = A(\eta_1)G_3(\eta_1, t_2) + \bar{A}(\eta_1)G_4(\eta_1, t_2) \tag{A4}$$

where $i = \sqrt{-1}$, $\overline{(\ \ )}$ denotes the complex conjugate, and

$$A(\eta_1) = \mu_1/[4\pi i(1-v_1)](a_r + ia_\theta)\, e^{i\omega_1}$$
$$B(\eta_2) = \mu_2/[4\pi i(1-v_2)](b_r + ib_\theta)\, e^{i(\pi+\omega_2)} \tag{A5}$$

and where

$$G_1 = -\delta\left(\frac{1}{(z-\bar{z}_2)} - \frac{\bar{z}_2 - z_2}{(\bar{z}-z_2)^2} + e^{2i\omega_2}\, \frac{\bar{z}_2 - \bar{z}}{(z-\bar{z}_2)^2}\right)$$

$$G_2 = -\delta\left(\frac{1}{\bar{z}-\bar{z}_2} - \frac{z_2 - \bar{z}_2}{(z-\bar{z}_2)^2} + e^{2i\omega_2}\, \frac{(z_2-\bar{z}_2)(z+\bar{z}_2 - 2\bar{z})}{(z-\bar{z}_2)^3}\right) - \frac{\Lambda}{z-\bar{z}_2}\, e^{2i\omega_2}$$

$$G_3 = \frac{1-\Delta_1}{z-z_1} + e^{2i\omega_2}\, \frac{\bar{z}_2(1-\delta_1) - \bar{z}(1-\Delta_1) + z_1(\delta_1 - \Delta_1)}{(z-z_1)^2}$$

$$G_4 = \frac{(1-\Delta_1)}{\bar{z}-\bar{z}_1} + e^{2i\omega_2}\, \frac{(1-\delta_1)}{z-z_1}$$

$$F_1 = -\delta_1\left(\frac{1}{z-\bar{z}_1} - \frac{\bar{z}_1 - z_1}{(\bar{z}-z_1)^2} + e^{2i\omega_1}\, \frac{(\bar{z}_1 - \bar{z})}{(z-\bar{z}_1)^2}\right)$$

$$F_2 = -\delta_1\left(\frac{1}{\bar{z}-z_1} - \frac{z_1 - \bar{z}_1}{(z-\bar{z}_1)^2} + e^{2i\omega_1}\, \frac{(z_1-\bar{z}_1)(z+\bar{z}_1 - 2\bar{z})}{(z-\bar{z}_1)^3}\right) - \frac{\Delta_1}{z-\bar{z}_1}\, e^{2i\omega_1}$$

$$F_3 = \frac{(1-\Delta)}{z-z_2} + e^{2i\omega_1}\, \frac{(1-\delta)\bar{z}_2 - \bar{z}(1-\Delta) - z_2(\Delta - \delta)}{(z-z_2)^2}$$

$$F_4 = \frac{(1-\Delta)}{\bar{z}-\bar{z}_2} + e^{2i\omega_1}\, \frac{(1-\delta)}{z-z_2}. \tag{A6}$$

In the above

$$\delta = \frac{\beta-\alpha}{1+\beta} \qquad \Delta = \frac{\alpha+\beta}{\beta-1} \tag{A7}$$

$$\delta_1 = \frac{\alpha-\beta}{1-\beta} \qquad \Delta_1 = \frac{\alpha+\beta}{1+\beta}. \tag{A8}$$

The semi-infinite reference crack corresponding to $0 \leqslant \eta_2 \leqslant \infty$ is represented by a distribution of dislocations $B(\eta_2)$, and the segment of crack corresponding to $0 \leqslant \eta_1 \leqslant a$ is represented by a distribution $A(\eta_1)$. The $B(\eta_2)$ and $A(\eta_1)$ are chosen such that the net tractions resulting from eqns (A1), (A2), (A3) and (A4) are zero everywhere on the crack surface. Since the a-dependence of the solution is known from dimensional considerations, a can be taken to be unity. The dual integral equations are then

$$2\int_0^\infty \frac{B(\eta_2)\,e^{i\omega_2}}{(\eta_2 - t_2)}\,d\eta_2 + \int_0^\kappa [B(\eta_2)G_1(\eta_2, t_2) + \bar{B}(\eta_2)G_2(\eta_2, t_2)]\,d\eta_2 + \int_0^{\pi_1}[A(\eta_1)G_3(\eta_1, t_2) + \bar{A}(\eta_1)G_4(\eta_1, t_2)]\,d\eta_1 = 0$$

$$2\int_0^1 \frac{\bar{A}(\eta_1)\,e^{i\omega_1}}{(t_1 - \eta_1)}\,d\eta_1 + \int_0^\kappa [B(\eta_2)F_3(\eta_2, t_1) + \bar{B}(\eta_2)F_4(\eta_2, t_1)]\,d\eta_2$$

$$+ \int_0^1 [A(\eta_1)F_1(\eta_1, t_1) + \bar{A}(\eta_1)F_2(\eta_1, t_1)]\,d\eta_1 = 0. \quad (A9)$$

With the changes of variables

$$\eta_2 = (1 + \xi_2)/(1 - \xi_2), \quad t_2 = (1 + u_2)/(1 - u_2). \quad (A10)$$

The integral equations (A9) can be rewritten as

$$\int_{-1}^1 \frac{\bar{D}(\xi_2)(1 - u_2)}{(\xi_2 - u_2)(1 - \xi_2)}\,d\xi_2 + \int_{-1}^1 [D(\xi_2)G_1(\eta_2, t_2) + \bar{D}(\xi_2)G_2(\eta_2, t_2)](1 - \xi_2)^{-2}\,e^{-i\omega_2}\,d\xi_2$$

$$+ \frac{1}{2}\int_0^1 [A(\eta_1)G_3(\eta_1, t_2) + \bar{A}(\eta_1)G_4(\eta_1, t_2)]\,e^{-i\omega_2}\,d\eta_1 = 0$$

$$\int_0^1 \frac{\bar{A}(\eta_1)\,d\eta_1}{(t_1 - \eta_1)} + \int_{-1}^1 [D(\xi_2)F_3(\eta_2, t_1) + \bar{D}(\xi_2)F_4(\eta_2, t_1)](1 - \xi_2)^{-2}\,e^{-i\omega_2}\,d\xi_2$$

$$+ \frac{1}{2}\int_0^1 [A(\eta_1)F_1(\eta_1, t_1) + \bar{A}(\eta_1)F_2(\eta_1, t_1)]\,e^{-i\omega_2}\,d\eta_1 = 0 \quad (A11)$$

where $D(\xi_2) = B(\eta_2)$. The representations of $A(\eta_1)$ and $D(\xi_2)$ for the different problems are constructed in Appendix B. The stress intensity factors at the tip of a deflected crack are given by

$$K_1 + iK_{II} = (2\pi)^{1/2}\,e^{i\omega_1}\lim_{\eta_1 \to 1}\{(1 - \eta_1)^{1/2}\bar{A}(\eta_1)\}. \quad (A12)$$

APPENDIX B: DISLOCATION REPRESENTATIONS

The representation of the dislocation distributions for the different problems are summarized here.

Problems A1 and B1

The remote field imposed on the semi-infinite crack is (3) in A1 and (15) in B1. Let $\delta = u(r, -\pi + \omega_2) - u(r, \pi + \omega_2)$ be the relative displacements of the crack faces associated with these fields. From the singularity analysis for the crack terminating at the interface, the remote dislocation distribution can be obtained from $b = d\delta/d\eta_2$ and eqn (A5) as

$$B(\eta_2) = c_0\eta_2^{-\lambda}k \quad (B1)$$

where $k \equiv k_1$ in A1, and $k \equiv k_1$ and $\lambda \equiv \lambda_1$ in B1. The complex constant c_0 is determined by the singularity analysis.

The most singular stresses in the vicinity of the kink of the crack (at $x = y = 0$) have the form $\bar{\sigma} \sim r^{-p}\bar{\sigma}(\theta)$ where, in general, p is a complex number depending on α, β, ω_1 and ω_2. Hein and Erdogan (1971) have obtained the equation for p. When $\beta = 0$, p is real. In the neighborhood of the kink $B \sim \eta_2^{-p}$ and $A \sim \eta_1^{-p}$.

The representation of $D(\xi_2)$ which builds-in the correct singularity at the kink and which approaches eqn (B1) remote from the interface is

$$D(\xi_2) = \left(\frac{1 - \xi_2}{2}\right)^\lambda \left(\frac{1 + \xi_2}{2}\right)^{-p}\left[c_0 k + (1 - \xi_2)\sum_{k=1}^m d_k T_{k-1}(\xi_2)\right] \quad (B2)$$

where the ds are complex coefficients which must be obtained in the solution and process and $T_j(\xi_2)$ is the Chebyshev polynomial of first kind of degree j. The representation for $A(\eta_1)$ is taken as

$$A(\eta_1) = \eta_1^{-p}(1 - \eta_1)^{-1/2}\sum_{j=1}^n a_j\eta_1^{j-1} \quad (B3)$$

and, by (A12), the stress intensity factors at the tip of the crack are

$$K_1 + iK_{II} = (2\pi)^{1/2}\,e^{i\omega_1}\sum_{j=1}^n \bar{a}_j. \quad (B4)$$

By substituting (B2) and (B3) into the two integral equation (A11) one obtains the two equations.

$$\sum_{k=1}^{m} [d_k E_{1k}(u_2) + \bar{d}_k F_{1k}(u_2)] + \sum_{j=1}^{n} [a_j G_{1j}(u_2) + \bar{a}_j H_{1j}(u_2)] = L_1(u_2) \qquad (B5)$$

$$\sum_{k=1}^{m} [d_k E_{2k}(t_1) + \bar{d}_k F_{2k}(t_1)] + \sum_{j=1}^{n} [a_j G_{2j}(t_1) + \bar{a}_j H_{2j}(t_1)] = L_1(t_1) \qquad (B6)$$

where integral expressions for E_{ik}, F_{ik}, G_{ij}, H_{ij} and L_i are readily identified. To determine the $m+n$ complex coefficients d_k and a_j, (B5) is satisfied at m Gauss–Legendre points on the interval $-1 < u_2 < 1$, and (B6) is satisfied at n Gauss–Legendre points on the interval $0 < t_1 < 1$. On the basis of numerical experimentation with various choices of m and n, the calculations were carried out with $m = n = 8$. We believe the results for the energy release rates reported in the figures are accurate to within about one percent. In the case of problem A1, symmetry implies that the real parts of d_k and a_j are zero.

Problem D1

The formulation of problem D1 is similar in most respects to B1 except that the concentrated wedge loads must be applied. This is accomplished by considering the solution for a concentrated force P acting on an otherwise traction-free boundary of a semi-infinite plane. The singular behavior of $N(\eta_2)$ near $\eta_2 = l$ must be consistent with this solution, i.e.

$$B(\eta_2) \to -P\,e^{i\omega_2}/[2\pi^2(\eta_2 - l)] \qquad (B7)$$

as $\eta_2 \to l$. The dislocation density remote from the wedge loading will have the form

$$B(\eta_2) \propto \eta_2^{-\lambda^*} \quad \text{for} \quad \eta_2 \to \infty \qquad (B8)$$

where λ^* is the eigenvalue of the problem in Section 3 which is the next larger than λ_1 and λ_2 in (14). This exponent characterizes the asymptotic outer solution to the semi-infinite crack problem for a loading which is confined to the vicinity of the tip.

A representation for $D(\xi_2)$ consistent with the above features and the singularity at the kink is

$$D(\xi_2) = (1 - \xi_2)^{\lambda^*}(1 + \xi_2)^{-p}\left[C(\xi_2 - \xi_0)^{-1} + \sum_{k=1}^{m} d_k T_{k-1}(\xi_2) \right] \qquad (B9)$$

where

$$C = -P\,e^{i\omega_2}\,(1 - \xi_0)^{2-\lambda^*}(1 + \xi_0)^p/(4\pi^2) \qquad (B10)$$

and $\xi_0 = (l-1)/(l+1)$. The representation for $A(\eta_1)$ is still given by eqn (B3). The integral equations reduce to the form given in (B5) and (B6), and the solution procedures are the same as described above. The results reported were computed with $m = n = 8$.

Problems A2, A3, B2 and D2

The formulation of these problems differs from their counterparts above only in that the portion of the crack beyond the kink lies along the interface. When $\beta = 0$, eqn (A3) gives the traction on the interface when $\omega_1 \to 0$ with $F_1 = 0$ and $F_2 = -(\delta_1 + \Delta_1)/(t_1 - \eta_1)$. The second integral equation in (A11) reduces to

$$(1-\alpha)\int_0^1 \frac{A(\eta_1)\,d\eta_1}{(t_1 - \eta_1)} + \int_{-1}^{1} [D(\xi_2)F_3(\eta_2, t_1) + \bar{D}(\xi_2)F_4(\eta_2, t_1)](1 - \xi_2)^{-2}\,d\xi_2 = 0. \qquad (B11)$$

The representations for $A(\eta_1)$ and $D(\xi_2)$ are still given by (B2) and (B3), and the interface stress intensity factors are given by

$$K_1 + iK_2 = (1-\alpha)(2\pi)^{3/2} \sum_{j=1}^{m} \bar{a}_j. \qquad (B12)$$

Problem C

The integral equation governing the dislocation distribution $B(\eta_2)$ for the wedge loaded crack approaching the interface is

$$2\int_0^L B(\eta)(\eta - t)^{-1}\,e^{i\omega_2}\,d\eta + \int_0^L [B(\eta)G_1(\eta, t) + \bar{B}(\eta)G_2(\eta, t)]\,d\eta = 0 \qquad (B13)$$

where η and t are zero at the crack tip. The distribution $B(\eta)$ must be consistent with the wedge loading (B7) and a square root singularity at the crack tip. The representation used is the same as that in (B9) and (B10) with $p = 1/2$. The integral equation is reduced to algebraic equations for the m complex coefficients d_k as in the previous problems. The results reported in Figs 7 and 9 were computed with $m = 20$ for $l/l_0 < 0.7$ and $m = 30$ for $l/l_0 \geqslant 0.7$.